NJC

Accepted Manuscript

ROYAL SOCIETY OF CHEMISTRY

rsc.li/njc

View Article Online
DOI: 10.1039/C9NJ01259A

ARTICLE

ESIPT-based fluorescent probe for cysteine sensing with large Stokes shift over homocysteine and glutathione and its application in living cells

Received 00th January 20xx,
Accepted 00th January 20xx

DOI: 10.1039/x0xx00000x

Peng Zhang[a], Yuzhe Xiao[a], Qian Zhang[a], Zixuan Zhang[a], Hongwei Yu[b] and Caifeng Ding[a*]

Cysteine (Cys) is an important amino acid containing a sulfhydryl group, which is involved in cellular growth, and Cys of abnormal level *in vivo* is suggestive of many diseases. Hence, development of fluorescent probes for intracellular Cys detection and imaging is of pivotal importance. So far, a number of fluorescence probes have been developed for Cys detection successfully. However, many of them could hardly discriminate Cys from Hcy, GSH or other reactive sulfur species (RSSs) and their emission wavelength of the probes is mainly located in ultraviolet/short region with small Stokes shifts (<100 nm). Herein, based on the impressive fluorescent properties of ESIPT progress, a new fluorescent probe named ABT-MVK is synthesized and used to detect Cys. This probe utilizes a typical ESIPT dye (HBT) as the fluorophore and an acrylate group as ESIPT blocking agent as well as recognition unit. Cleavage of acrylate moiety can be achieved by Cys rapidly and specifically in aqueous buffer, which leads to restoring ESIPT process and endows the probe with a "Turn ON" fluorescent detection procedure with large Stokes shifts (*ca.* 225 nm) for Cys with superior selectivity over various potential interferences, including Hcy, GSH, Na_2S or $NaHSO_3$. The detection limit for Cys was calculated to be as low as 19 nM and intracellular bio-imaging of Cys by this probe was successfully applied in living cells, indicative of great potential for biological applications.

Introduction

Intracellular reactive sulfur species (RSSs), including hydrogen sulfide, thiols, persulfides, polysulfides and S-modified cysteine adducts such as S-nitrosothiols and sulfenic acids, are generally considered to be sulfur-containing biomolecules, which play essential roles in mediating physiological processes and balancing biological systems. [1-3] Clinical studies demonstrated that even though structural frameworks of these RSSs are similar, they are related to different physiological and pathological processes. [4-8] Changes in the levels of these RSSs are linked to many diseases. For example, cysteine (Cys), as an important amino acid containing sulfhydryl group, plays vital roles in many significant cellular functions. [9, 10] Cys (30–200 μM) of normal levels serves as the source of sulfide in protein synthesis, detoxification and human metabolism. [11] However, Cys of abnormal levels in living cells is usually associated with certain diseases including skin lesions, rheumatoid arthritis, liver damage and Parkinson's disease. [12-13] Hence, developing a handy and valid method for Cys sensing and imaging in living system is crucial.

In recent years, detection of RSSs has gained considerable attention, and available techniques at present for bio-thiols detection include colorimetric method, [14, 15] electrochemical method, [16-18] mass spectrometry [19-21] and high performance liquid chromatography (HPLC) [22-24]. However, these detection methods require the living biosamples to be post-mortem processed. Thus, they are destructive and not suitable for monitoring biothiols in native biological environments. Among the present detection techniques, fluorescent analysis is particularly attractive, contributed by its facile design, high sensitivity, low budget, and great feasibility for bioimaging. [25-32] Although a series of fluorescent schemes have been built up for fluorescent detection of amino acid and biothiols until now, most of them exhibited low selectivity for Cys. [33-37] A major problem for those reported probes is that they could barely discriminate Cys from other RSSs such as homocysteine (Hcy), glutathione (GSH) and even S^{2-}, HSO_3^-, as these biothiols possess similar structures and reactivity. Besides, the higher intracellular level of GSH (1-10 mM) than that of Cys [38] amplified the difficulty of specific detection for Cys over GSH. Notably, these biothiols play different pivotal biological roles, so clear discrimination of Cys from Hcy and GSH would make sense to exploring their complicated function. [39, 40] In fact, up to now only a few fluorescent probes were reported to be able to detect Cys with improved selectivity over Hcy, GSH, and so on. [41-46] Nevertheless, many of the reported probes generally

[a] *Key Laboratory of Optic-electric Sensing and Analytical Chemistry for Life Science, MOE; Shandong Key Laboratory of Biochemical Analysis; Key Laboratory of Analytical Chemistry for Life Science in Universities of Shandong; College of Chemistry and Molecular Engineering. Qingdao University of Science and Technology, Qingdao 266042, PR China. E-mail: dingcaifeng2003@163.com.*
[b] *Qingdao Municipal Center for Disease Control & Prevention, Qingdao 266033, PR China.*

Electronic Supplementary Information (ESI) available: fluorescence, absorption and NMR spectral profiles. See DOI: 10.1039/x0xx00000x

display some disadvantages such as tedious synthesis routes and small Stokes shifts (< 100 nm). Therefore, it has been of focus and difficulty to construct fluorescence probes with superior properties for the detection of Cys.

ESIPT-active fluorescent dyes have been widely used to construct fluorescent probes with large Stokes shift. [47-51] 2-(2′-Hydroxyphenyl)-benzothiazoles (HBT), as a typical class of ESIPT fluorescent dyes, have been utilized as the scaffold to design fluorescent probes for the detection of many species with a large Stokes shift. Particularly, extension of the π-conjugation of HBT at the ortho- or para-position of the phenol can afford fluorescent probes with red/NIR emission, which made the probes more suitable for biological imaging. [52, 53]

In view of the aforementioned reasons, we report a facile prepared HBT-based fluorescent probe (ABT-MVK) with large Stokes shift and high selectivity for Cys sensing in this work, in which an acrylate group was introduced as the reaction site for Cys and HBT acted as an ESIPT active group. In order to achieve the redder emission, conjugation of HBT was prolonged at the ortho- position of the phenol moiety by Aldol reaction. Notably, our research found that this probe governed several impressive sensing properties compared to the reported Cys probes (Table S1). First and the most important of all, the probe is highly selective for Cys over other diverse anions, cations and amino acids including Hcy, GSH, S^{2-} and HSO_3^-. Second, it offers a rapid (within a few minutes) and sensitive detection process for Cys in aqueous buffer with a red fluorescence "turn-on" signal output and a relatively low detection limit at nanomolar level (19 nM). Third, this probe is simple with easy and convenient synthesis, readily available and visible-light-excitable with a large Stokes shift (*ca.* 225 nm), and can be used for fluorescence imaging of exogenous and endogenous Cys in living cells with low cytotoxicity. All these merits indicate that the new probe appears to be a rather promising fluorescent probe for Cys.

Results and discussion

Design and synthesis of probe ABT-MVK

To design a feasible fluorescence probe for detecting Cys selectively with larger Stokes shift, the traditional ESIPT active group HBT was employed as fluorophore framework, to which an acrylate group was introduced as the binding site, and its conjugation was prolonged at the ortho- position of the phenol by Aldol reaction to achieve a red emission. The probe was synthesized by simple reaction of HBT-MVK and acryloyl chloride in the presence of triethylamine in CH_2Cl_2 (Scheme 1), it was fully characterized by standard spectroscopic techniques including ^{1}H NMR, ^{13}C NMR and HR-MS. It is noteworthy that the preparation could be achieved readily and tedious purification procedures are avoided.

The optical property of the ESIPT-based fluorescent probe ABT-MVK and the feasibility study was first investigated. As shown in Figure 1, 10 μM ABT-MVK in PBS buffer (10 mM, pH 8.0) shows a maximum absorption at 290 nm and emits

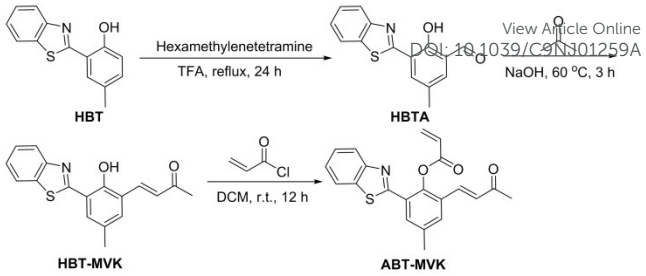

Scheme 1. Synthesis route of ABT-MVK.

negligible fluorescence ("off" state) as a result of the quenching effect by acrylate group. The spectroscopic response of ABT-MVK (10 μM) to Cys was examined under this condition. After addition of 40 μM Cys, the absorption centered at 290 nm decreased accompanied by a new absorption at 370 nm originating from of n-π transition with an isosbestic point at 334 nm (Figure 1a). Accordingly, the fluorescence intensity at 595 nm increased by 73-fold with a quantum yield of 0.10 ("on" state) when it was excited at 370 nm (Figure 1b), exhibiting a large Stokes shift of *ca.* 225 nm. Based on the above principles, a simple visible-light-excitable ESIPT-based probe for selective "turn-on" detection of Cys in aqueous solution was thereby developed.

Sensing condition optimization

To construct a sensitive fluorescent probe for Cys, the sensing conditions usually need to be optimized. The effect of pH on the emission intensity of ABT-MVK and the reaction solutions of ABT-MVK toward RSSs was first evaluated. 10 mM PBS buffer solutions of pH ranging from 5.5 - 9.5 were investigated. Referring to the results shown in Figure 2, for ABT-MVK only, the emission intensity at 595 nm did not change within the investigated pH range, indicating that ABT-MVK showed relative stability under the experimental pH conditions. While ABT-MVK was treated with 40 μM Cys, significant fluorescent enhancement at 595 nm could be observed in the pH range of 7.0-9.0. When it was applied to other biothiols (Hcy or GSH) of the same concentration, the fluorescence of ABT-MVK hardly

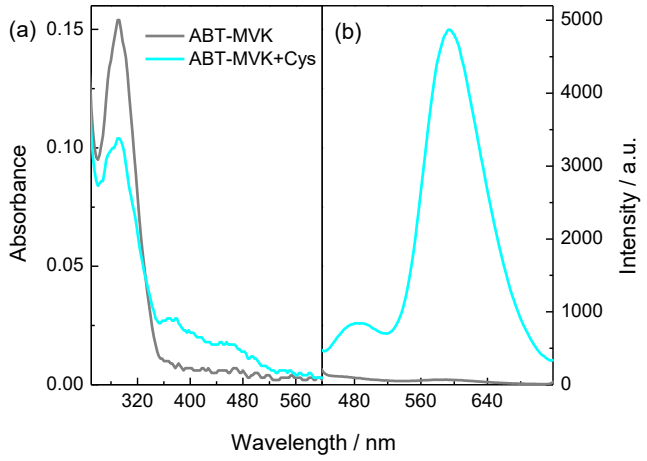

Fig. 1. Absorption (a) and fluorescence (b) spectra of ABT-MVK without (gray line) and with (cyan line) 40 μM Cys in 10 mM PBS buffer of pH 8.0. [ABT-MVK] = 10 μM, λ_{ex} = 370 nm.

View Article Online
DOI: 10.1039/C9NJ01259A

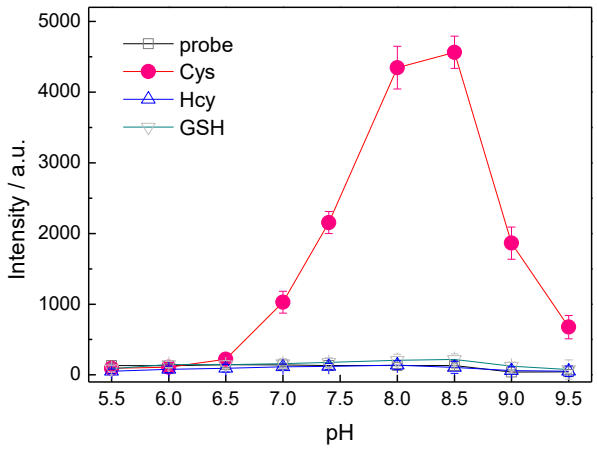

Fig. 2. Plots of intensity of ABT-MVK at 595 nm without (black squares) or with 40 μM Cys (red dots), Hcy (blue triangles) and GSH (gray triangles) versus solution pH from 5.5 to 9.5 incubated for 10 min. Solution pH was tuned by 10 mM phosphate buffer. [ABT-MVK] = 10 μM, λ_{ex} = 370 nm.

changed. These results implied that ABT-MVK could be applied to detect Cys in physiological circumstances with high selectivity.

To obtain the appropriate reaction time of ABT-MVK and Cys, time-dependent fluorescence of ABT-MVK (10 μM) with 4 equivalents Cys was investigated by measuring fluorescence intensity changes at 595 nm every 1 minute. As shown in Figure 3, fluorescence intensity at 595 nm increased immediately and levelled off within 10 minutes after Cys was added (Figure 3a). However, free ABT-MVK (10 μM) emission was negligible during the same observation time (Figure S5). The results suggest that ABT-MVK could rapidly respond to Cys. In the vivid contrast against Cys, under the same conditions, fluorescence changes of ABT-MVK upon addition of other RSS (Hcy, GSH, Na_2S or $NaHSO_3$) are almost negligible within observation time in 24 minutes (Figure 3b). As a result, it is affirmed that ABT-MVK shows a highly selective response to Cys over Hcy, GSH, Na_2S and $NaHSO_3$, indicating its potential usage for selective Cys detection in biosystems.

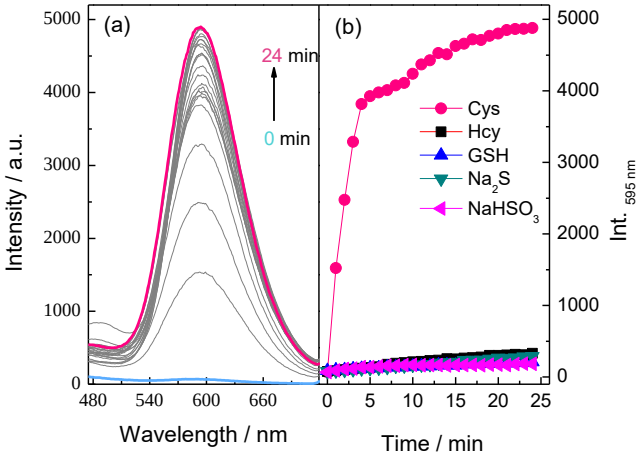

Fig. 3. (a) Time-dependent fluorescence spectra of ABT-MVK incubated from 0 to 24 min upon addition of 40 μM Cys in 10 mM PBS buffer (pH =8.0). (b) Intensity of ABT-MVK at 595 nm after addition 40 μM RSSs from 0 to 24 min in 10 mM PBS buffer (pH =8.0). [ABT-MVK] = 10 μM, λ_{ex} = 370 nm.

Recognition performance of ABT-MVK for Cys

Response of ABT-MVK towards Cys of varying concentrations was investigated in 10 mM PBS buffer pH 8.0. ABT-MVK alone was almost no emission because of the quenchment of acrylate group. However, upon increasing concentration of Cys from 0 to 40 μM, a sensitive fluorescent response toward Cys was observed (Figure 4a), by a rapid enhancement of the red emission with a maximum wavelength at 595 nm. When 15 μM Cys was added, the fluorescence intensity of ABT-MVK at 595 nm increased by *ca.* 73-fold comparing with that of the original ABT-MVK solution (Figure 4a inset). It is understandable that Cys could effectively eliminate the acrylic ester moiety in ABT-MVK to generate the chromophore HBT-MVK with red emission based on ESIPT process. Job plots showed that ABT-MVK to Cys stoichiometry was 1:1 (Figure S6), which also confirmed the abovementioned reaction mechanism. The fluorescence intensity at 595 nm increased linearly with Cys concentration over 0 to 15 μM (y=309.6x-2.06, R^2=0.995, Figure 4a inset and Figure S7), [54, 55] giving a detection limit of 19 nM in terms of 3σ/k, in which σ is the standard deviation of 11 blank measurements and k is the linear slope

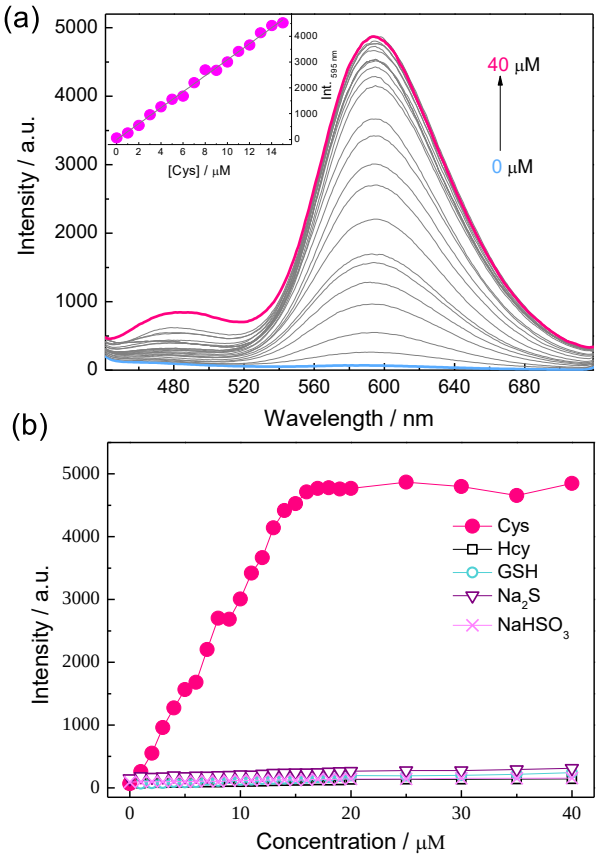

Fig. 4. (a) Fluorescence spectra of ABT-MVK in 10 mM PBS buffer of pH 8.0 in the presence of increasing concentration of Cys from 0 to 40 μM. (b) Plots of intensity at 595 nm of ABT-MVK versus RSSs concentration from 0 to 40 μM. [ABT-MVK] = 10 μM, λ_{ex} = 370 nm.

View Article Online DOI: 10.1039/C9NJ01259A

of the dependence of intensity of ABT-MVK at 595 nm versus Cys concentrations.[56] The above results indicate that ABT-MVK can be readily applied for quantitative detection of Cys with high sensitivity in aqueous medium.

Proposed mechanism of ABT-MVK with Cys

The fluorescent enhancement of ABT-MVK caused by Cys was mainly due to the eliminated acrylic ester moiety. The reaction between biothiols and acrylate group has been well studied so far. [57-60] Referring to these reported literatures and our experimental results, proposed detection mechanism of probe ABT-MVK for Cys was shown in Scheme 2. The reaction first underwent by a conjugate addition of Cys to α, β-unsaturated carbonyl group of ABT-MVK to generate the corresponding thioether, a transient intermediate which could subsequently proceed an intramolecular cyclisation to afford the free chromophore HBT-MVK. As shown in the above experiments, ABT-MVK exhibits high selectivity for Cys over GSH and Hcy. It could be illustrated by the fact that Cys exhibits faster reaction kinetics than GSH and Hcy in the process of intramolecular cyclisation, because the formation of seven-membered ring product was more favorable in kinetics. To prove the speculation, HR-MS spectrometry analysis was displayed, signal at m/z 310.0886 (calcd. 310.0896) for compound HBT-MVK ($[C_{18}H_{15}NO_2S+H]^+$) in the mixture of ABT-MVK/Cys was found, that matched well with the theoretical simulation (Figure S8).

Moreover, ^{1}H NMR spectra of ABT-MVK, ABT-MVK-Cys reaction solution and HBT-MVK were further examined to verify the abovementioned mechanism (Figure 5). As shown in Figure 5, after the reaction of HBT-MVK with Cys, the characteristic proton signals of acrylate group of HBT-MVK (signals j, l, k) at 6.64, 6.35 and 6.68 ppm disappear and the proton signals in aromatic region are consistent with that of HBT-MVK. The above results supported the proposed reaction mechanism between ABT-MVK and Cys.

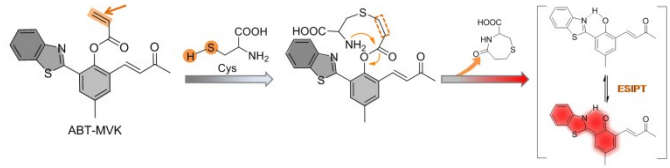

Scheme 2. Proposed response mechanism for ABT-MVK to Cys.

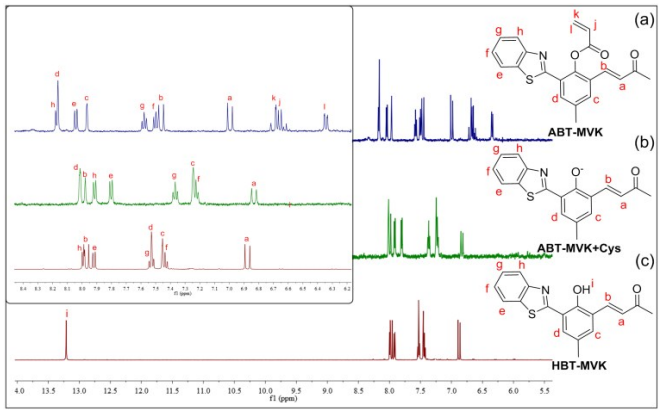

Fig. 5. Partial ^{1}H NMR (500 MHz) spectra of (a) ABT-MVK (5.0 mM), (b) ABT-MVK with 1.5 equivalents of Cys and (c) HBT-MVK measured in DMSO-d_6. Inset: A partially enlarged view of ^{1}H NMR (500 MHz) spectra. [ABT-MVK] = [HBT-MVK] = 5.0 mM.

The selectivity and competition studies

To examine the high selectivity of ABT-MVK toward Cys, the effect of other biologically relevant analytes was then evaluated. The fluorescence spectrum of HBT-MVK was measured in the presence of various anions (F^-, Cl^-, I^-, AcO^-, NO_3^-, CO_3^{2-}, S^{2-} and HSO_3^- as shown in Figure 6a), cations (Na^+, K^+, Mg^{2+}, Ca^{2+}, Ni^{2+}, Zn^{2+}, Co^{2+}, Pb^{2+}, Fe^{3+}, Al^{3+} and Cu^{2+} as shown in Figure 6b) and amino acids (Ala, Asp, Gln, Glu, Gly, His, Ile, Leu, Lys, Met, Pro, Ser, Thr, Val, Hcy, GSH and Cys as shown in Figure 6c). It was found that only addition Cys influenced the emission of ABT-MVK. Excess amount (10 equivalents) of those foreign compounds did not change the fluorescence of ABT-MVK at 595 nm, further confirming the high selectivity to Cys. Moreover, these results clearly showed that ABT-MVK was highly selective for Cys over Hcy, GSH, Na_2S and $NaHSO_3$, which deserves considerable attention, because so far highly selective fluorescent probes for Cys are relatively rare, as mentioned above. As for the sensing strategy present herein, the Michael addition/cyclisation procedure between acrylic ester and Cys generally exhibited faster reaction kinetics than Hcy and GSH. [61-64] The competitive experiments were also implemented to investigate the fluorescent behavior of ABT-MVK with Cys in the presence of various species mentioned above (Figures S9-S11). The results indicated that Cys can be well detected even in the presence of other anions, cations and amino acids except Cu^{2+}. The fluorescence quenching induced by Cu^{2+} may be due to the coordination of copper ions with the product (HBT-MVK) of ABT-MVK and cysteine. Fortunately, fluorescent response to Cu^{2+} can be

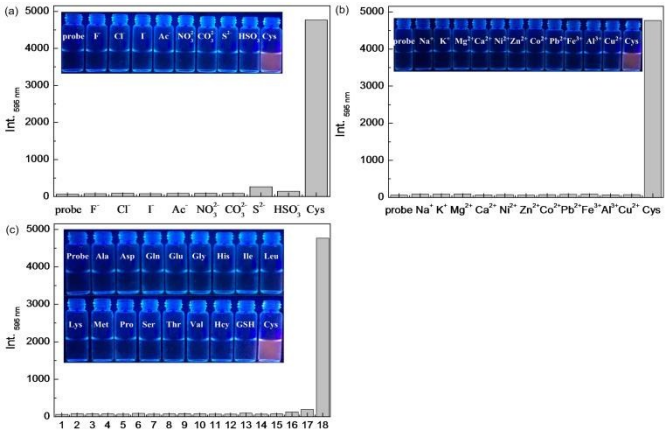

Fig. 6. Fluorescence intensity of ABT-MVK at 595 nm in 10 mM PBS buffer of pH 8.0 in the presence of 100 μM anions (a, free, F^-, Cl^-, I^-, AcO^-, NO_3^-, CO_3^{2-}, S^{2-}, HSO_3^- and Cys), cations (b, free, Na^+, K^+, Mg^{2+}, Ca^{2+}, Ni^{2+},Zn^{2+}, Co^{2+}, Pb^{2+}, Fe^{3+}, Al^{3+}, Cu^{2+} and Cys) and amino acids (c, 1-18: Free, Ala, Asp, Gln, Glu, Gly, His, Ile, Leu, Lys, Met, Pro, Ser, Thr, Val, Hcy, GSH and Cys). Inset: Photographs of before mentioned solutions taken under the irradiation of 365 nm UV light. [ABT-MVK] = 10 μM, λ_{ex} = 370 nm.

masked upon the usage of EDTA as a coadditive (Figure S12). These above results indicated that ABT-MVK could selectively distinguish Cys from GSH, Hcy and other biologically relevant analytes.

Cytotoxicity assay and fluorescence imaging in living cells

For intracellular fluorescent imaging, cytotoxicity of the probe is a critical consideration. Thus, we evaluated the cell cytotoxicity of ABT-MVK by CCK8 analysis for HeLa cells afterward. As shown in Figure S13, HeLa cells viability remained above 80% after being incubated with 2-50 μM of ABT-MVK for 2 h, which suggested that the probe exhibited limited cytotoxicity to living cells under the experimental conditions, and hold great potential for biological applications. Based on the above research, the practical applications of ABT-MVK for fluorescent imaging of intracellular Cys in living cells was investigated. As revealed in Figure 7, when HeLa cells were incubated with 10 μM ABT-MVK for 30 min, the cells started to show bright red fluorescence (A1). However, when cells were pretreated with 1.0 mM N-ethylmaleimide (NEM), which is a well known thiol trapping reagent, before cultured with probe ABT-MVK, little fluorescence was seen in the observation window (B1). As another control experiment, after HeLa cells were treated with NEM, exogenous Cys (100 μM), and ABT-MVK for 30 min sequentially, the red fluorescence was also observed (C1). In contrast, when HeLa cells went similar treatment scheme with NEM, Hcy (100 μM) or GSH (100 μM) followed by incubation with ABT-MVK for another 30 min respectively, red fluorescence can hardly be visualized (D1 and E1). The results demonstrate that ABT-MVK possesses good membrane permeability and is able to detect intracellular Cys in living cells.

As the intracellular Cys level is known to associate with oxidative stress, the investigation of the probe in response to

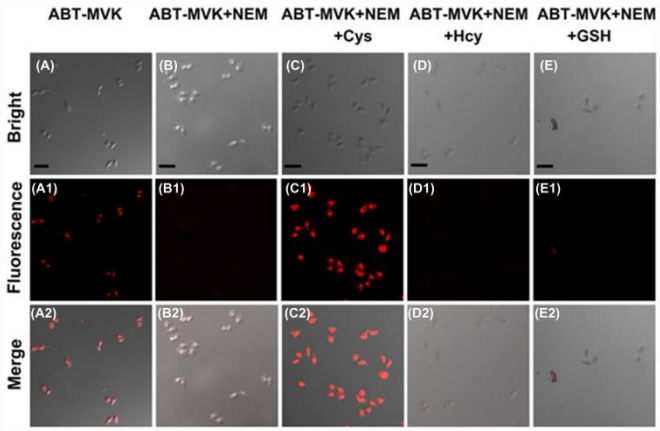

Fig. 7. Confocal microscopy fluorescence images of Cys in living HeLa cells. (A) HeLa cells incubated with ABT-MVK (10 μM) for 30 min. (B) HeLa cells pretreated with NEM (1.0 mM) for 30 min and then incubated with ABT-MVK (10 μM) for 30 min. (C, D, E) HeLa cells pretreated with NEM (1.0 mM) for 30 min and then incubated with Cys, Hcy, and GSH (100 μM) for 30 min, respectively, and finally incubated with ABT-MVK (10 μM) for 30 min. Top: bright field, middle: fluorescent field, bottom: merged field. λ_{ex} = 405 nm, λ_{em} = 550-650 nm. Scale bar: 50 μm.

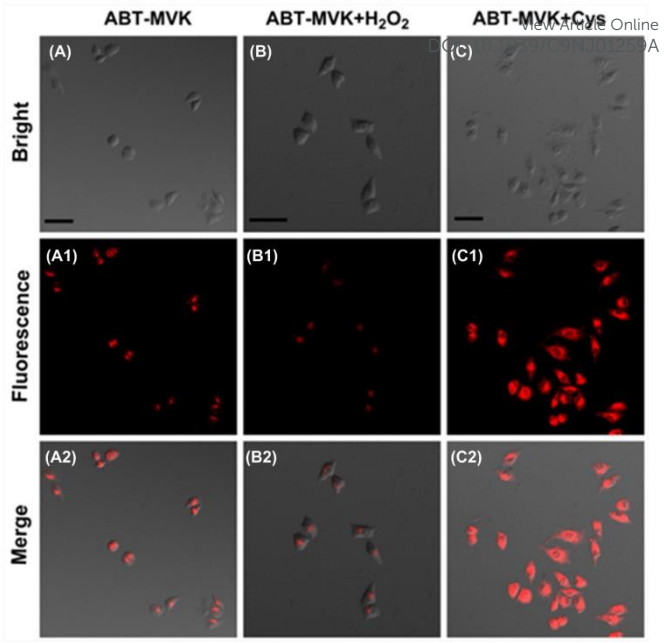

Fig. 8. Confocal microscopy fluorescence images of (A) HeLa cells incubated with ABT-MVK (10 μM) for 30 min; (B) HeLa cells pretreated with H_2O_2 (200 μM) for 30 min and then incubated with ABT-MVK (10 μM) for 30 min; (C) HeLa cells pretreated with Cys (100 μM) for 30 min and then incubated with ABT-MVK (10 μM) for 30 min. Top: bright field, middle: fluorescent field, bottom: merged field. λ_{ex} = 405 nm, λ_{em} = 550-650 nm. Scale bar: 50 μm.

the change of Cys concentration in living cells was demonstrated by altering the redox balance. When the HeLa cells were pretreated with 200 μM H_2O_2 for 30 min before incubation with ABT-MVK (10 μM), there was a dramatic decrease observed in red fluorescence (Figure 8B) compared with those without H_2O_2 pretreatment (Figure 8A). However, cells pretreated with exogenous 100 μM cysteine rather than H_2O_2 showed the strongest red fluorescence (Figure 8C). Such changes in fluorescence acted as response to the decrease of intracellular Cys concentration arising from the Cys oxidation by H_2O_2. Therefore, these findings suggested that ABT-MVK probe could be used as a tool to track the level of intracellular Cys.

Conclusions

In summary, we have developed a new type of ESIPT-based fluorescent probe, ABT-MVK, for detecting Cys. The probe was easily synthesized by using a traditional ESIPT unit HBT as fluorophore, the conjugation of which was prolonged by Aldol reaction to achieve a red emission, and an acrylate group was introduced as a binding site for Cys. The probe itself was almost non-fluorescent ("off" state) due to the quenching effect from acrylate group. When Cys was introduced, the fluorescence enhancement degree of ABT-MVK estimated at 595 nm was more than 73-fold ("on" state), which arose from the Michael addition/cyclisation sequence mechanism and

View Article Online DOI: 10.1039/C9NJ01259A

exhibited a large Stokes shift of *ca.* 225 nm upon excitation at 370 nm. Most importantly, the probe showed a rapid, sensitive and selective fluorescent sensing proposal for Cys in aqueous buffer over various potential interferences including Hcy, GSH, Na_2S and $NaHSO_3$. In addition, this probe possessed low cytotoxicity and well-behaved membrane permeability, allowing it to be applied for detecting Cys in living cells. As a result, this fluorescent probe would be practically useful and greatly beneficial to investigate and monitor Cys in living biological systems.

Experimental section

Reagents and instruments

All reagents and solvents utilized in organic syntheses were purchased from Aladdin reagent (Shanghai) co., Ltd and were used as received. Cervix carcinoma (HeLa cells) were provided by FDCC (Shanghai, China). Buffer solutions for spectral investigation herein were prepared by triple-distilled water.

Silica gel plates were used for thin layer chromatography (TLC) and silica gel of 200-300 mesh was applied for column chromatography. ^{1}H NMR and ^{13}C NMR spectra were recorded by Bruker AV500 or AV600 NMR spectrometer using DMSO-d_6 as solvent. Chemical shifts were reported in parts per million (ppm) downfield from tetramethylsilane (TMS, as internal standards, δ=0 ppm). High-resolution mass spectra (HRMS) were measured by a FT-ICR-MS mass spectrometer. Absorption spectra were obtained on a UH5300 UV-Vis spectrophotometer. Fluorescence spectral measurements were operated on a Hitachi F-4600 spectrophotometer, and the excitation and emission slits were both set at 5 nm. All the spectra were measured using a 1-cm quartz cell. Cellular imaging by laser scanning confocal microscopy was carried out on Leica SP5 Point Scanning Confocal. Additionally, the cytotoxic effect of the probe was examined by Cell Counting Kit-8 (CCK-8, purchased from Sigma-Aldrich and used as received) assay using Bio-Tek ELX800 microplate reader.

Synthesis of the probe

Synthesis of HBT. 2-(2-Hydroxyphenyl)-benzothiazole (HBT) was synthesized according to the literature. [65]

Synthesis of HBTA. 0.432 g (2.0 mmol) 2-(2-Hydroxyphenyl)-benzothiazole (HBT) and 0.840 g (6.0 mmol) hexamethylenetetramine were dissolved in 20 mL TFA. The contents were heated at reflux with stirring for 24 h after which the heating was discontinued and allowed to cool to room temperature. The solution was neutralized by 1 N of NaOH, and the precipitate generated was filtered and washed with water. And then purification of the residue on a silica gel column (CH_2Cl_2 and MeOH 100 : 1, v/v) furnished the pure product (0.404 g) in 82% yield. ^{1}H NMR (500 MHz, DMSO-d_6) δ (ppm) 12.75 (s, 1H), 10.32 (s, 1H), 8.20 (d, J = 7.9 Hz, 2H), 8.11 (d, J = 8.1 Hz, 1H), 7.72 (d, J = 1.3 Hz, 1H), 7.58 (t, J = 7.6 Hz, 1H), 7.50 (t, J = 7.5 Hz, 1H), 2.38 (s, 3H).

Synthesis of HBT-MVK. 0.400 g (1.5 mmol) HBTA was dissolved in 20 mL acetone and the solution was heated at 50 °C. Then 2 mL of 10 % sodium hydroxide solution was dropped slowly, and the contents were heated at 50 °C with stirring for another 4 h, after which cooled to r.t. and neutralized by 3 N of HCl, the precipitate was filtered and washed with water 3 times. At last purification of the obtained power on a silica gel column (CH_2Cl_2 and MeOH 80 : 1, v/v) furnished the pure product (0.280 g) in 60% yield. ^{1}H NMR (500 MHz, DMSO-d_6) δ (ppm) 12.96 (s, 1H), 8.20 (d, J = 8.0 Hz, 1H), 8.11 (d, J = 8.1 Hz, 1H), 7.86 (d, J = 16.4 Hz, 1H), 7.77 (s, 1H), 7.73 (s, 1H), 7.59 (t, J = 7.6 Hz, 1H), 7.51 (t, J = 7.5 Hz, 1H), 6.96 (d, J = 16.4 Hz, 1H), 2.34 (d, 6H).

Synthesis of ABT-MVK. Compound HBT-MVK (0.155 g, 0.5 mmol) was dissolved in CH_2Cl_2 (30 mL) with 100 μL TEA and stirred at 0 °C. Acryloyl chloride (100 μL) was added slowly though syringe. After that, the reaction solution was stirred at r. t. for another 4 h. Then, the solution was concentrated under reduced pressure. After being purified by the silica gel chromatography (CH_2Cl_2/MeOH, 100 : 1, v/v), compound ABT-MVK was obtained as a light yellow solid (0.138 g, 76%). ^{1}H NMR (600 MHz, DMSO-d_6) δ (ppm) 8.18 (d, J = 7.7 Hz, 2H), 8.05 (d, J = 8.0 Hz, 1H), 7.97 (s, 1H), 7.60 – 7.57 (m, 1H), 7.52 – 7.49 (m, 1H), 7.47 (d, J = 16.2 Hz, 1H), 7.00 (d, J = 16.2 Hz, 1H), 6.72 – 6.68 (m, 1H), 6.67 – 6.62 (m, 1H), 6.35 (dd, J = 10.0, 1.5 Hz, 1H), 2.49 (s, 3H), 2.32 (s, 3H); ^{13}C NMR (151 MHz, DMSO-d_6): δ (ppm) δ 197.48, 164.01, 161.41, 152.16, 144.29, 136.82, 135.80, 134.95, 134.35, 131.93, 130.56, 129.78, 128.51, 126.96, 126.72, 126.32, 125.82, 122.89, 122.10, 27.97, 20.23. ESI-MS *m/z*: $[M+Na]^+$ Calcd for $C_{21}H_{17}NO_3SNa^+$ 386.0821; Found 386.0811.

General procedures for spectra measurements

The stock solutions of ABT-MVK (5.0 mM) and N-ethylmaleimide (NEM, 100 mM) were prepared in HPLC-grade DMSO and stored at 4 °C. Stock solutions of 10 mM RSSs, anions (sodium salts), cations (chloride salts) and amino acids were prepared by direct dissolution in deionized water. Absorption and fluorescence measurements were carried out using the stock solution of ABT-MVK in DMSO, which was diluted by 10 mM PBS buffer of required pH, to afford the desired concentration of ABT-MVK at 10 μM, to which Cys or other guest species were added.

Detection limit

The detection limit of Cys (3σ/k) was calculated based on the linear relationship between the intensity at 595 nm and its concentration, where σ is the standard deviation of the blank measurements (n=11) and k is the slope of the linear dependence of intensity versus Cys concentration.

Cell cytotoxicity study

To study the cytotoxicity of the probe, HeLa cells were seeded at 6×10^4 cells per well in 96-well plates and incubated for 24 h before the treatment, followed by exposure with different concentrations (2-50 μM) of probe ABT-MVK for 4 h. After being washed with Dulbecco's Phosphate Buffered Saline (DPBS), the cells were incubated for further several hours, and then the cytotoxic effects of ABT-MVK were determined using Cell Counting kit-8 (CCK-8) assays.

Cell culture and fluorescent imaging

HeLa cells were seeded in high-glucose DMEM supplemented with 10 % fetal bovine serum, 1 % streptomycin and 1 % penicillin. Cultures were maintained in a humidified incubator at 37 °C, in 5 % CO_2 / 95 % atmosphere. For intracellular Cys imaging, the cells were incubated with 10 μM ABT-MVK (with 0.2% DMSO, v/v) for 30 min at 37 °C and washed three times with PBS buffer for imaging immediately. For NEM-treated experiments, HeLa cells were pretreated with 1.0 mM NEM for 30 min at 37 °C, washed three times with PBS buffer, and incubated with 10 μM ABT-MVK (or incubated with 100 μM Cys, Hcy or GSH for 30 min prior to addition of ABT-MVK) for 30 min at 37 °C. The cell imaging was carried out after they were washed with PBS. For H_2O_2-treated experiments, HeLa cells were pretreated with 200 μM H_2O_2 for 30 min at 37 °C, washed with PBS buffer, and incubated with 10 μM ABT-MVK for 30 min. Cell imaging was carried out after washing cells with PBS. Fluorescence imaging of HeLa cells was performed on Leica SP5 Point Scanning Confocal fluorescence microscope with excitation wavelength fixed at 405 nm and fluorescence wavelengths in the range of 550 - 650 nm.

Conflicts of interest

There are no conflicts to declare.

Acknowledgements

This work was supported by the National Natural Science Foundation of China (21375070, 21422504), the Fund Project for Shangdong Key R&D Program (2017GGX20121), and the support from Key Laboratory of Spectrochemical Analysis & Instrumentation (Xiamen University), Ministry of Education (SCAI1702, SCAI1703).

Notes and references

1 M. C. H. Gruhlke, A. Slusarenko, *Plant Physiol. Biochem.*, 2012, **59**, 98−107.
2 G. I. Giles, C. Jacob. *Biol. Chem.*, 2002, **383**, 375–388.
3 K. G. Reddie, K. S. Carroll. *Curr. Opin. Chem. Biol.,* 2008, **12**, 746–754.
4 C. E. Paulsen, K. S. Carroll. *Chem. Rev.*, 2013, **113**, 4633–4679.
5 H. J. Forman, H. Q. Zhang, *A. Rinna, Mol. Aspect. Med.*, 2009, **30**, 1–12.
6 A. R. Rosa, N. Singh, E. Whitaker, M. deBrito, A. M. Lewis, E. Vieta, G. C. Churchill, J. R. Geddes and G. M. Goodwin. *Psychol. Med*., 2014, **44**, 2409–2418.
7 C. Perricone, C. D. Carolis, R. Perricone, *Autoimmun. Rev.*, 2009, **8**, 69–701.
8 S. Seshadri, A. Beiser, J. Selhub, P. F. Jacques, I. H. Rosenberg, R. B. D'agostino, P. W. Wilson, P. A. Wolf. *New Engl. J. Med*., 2002, **346**, 476–483.
9 K. G. Reddie, K. S. Carroll. Curr. Opin. *Chem. Biol.*, 2008, **12**, 746−754.
10 H. T. Zhang, R. C. Liu, J. Liu, L. Li, P. Wang, S. Q. Yao, Z. T. Xu and H. Y. Sun. *Chem. Sci*., 2016, **7**, 256–260.
11 M. W. Lieberman, A. L. Wiseman, Z. Z. Shi, B. Z. Carter, R. Barrios, C. N. Ou, P. Chévez-Barrios, Y. Wang, G. M. Habib, J. C. Goodman, S. L. Huang, R. M. Lebovitz and M. M. Matzuk. *Proc. Natl. Acad. Sci. U. S. A*., 1996, **93**, 7923–7926.
12 T. Koopmans, M.van Haren, van L. Q. Ufford, J. M. Beekman, N. I. Martin. Bioorg. *Med. Chem.,* 2013, **21**, 553–559.
13 W. Y. Feng, M. X. Li, Y. Sun, G. Q. Feng. *Anal. Chem.*, 2017, **11**, 6106–6112.
14 Y. Xu, Y. Sun, Y. Zhang, C. Lu, J. Miao, *Zhejiang Univ. Sci. B.,* 2016, **17**, 807–812.
15 C. Wu, D. Fan, C. Zhou, Y. Liu, E. Wang, *Anal. Chem.*, 2016, **88**, 2899–2903.
16 R. Thota, V. Ganesh, *Rsc. Adv.*, 2016, **6**, 49578–49587.
17 S. Shahrokhian, *Anal.Chem*., 2001, **73**, 5972–5978.
18 S. Wu, X. Lan, F. Huang, Z. Luo, H. Ju, C. Meng, C. Duan, *Biosens. Bioelectron.*, 2012, **32**, 293–296.
19 A. Kranawetvogl, F. Worek, H. Thiermann, H. John, *Rapid Commun. Mass Sp.,* 2016, **30**, 2191–2200.
20 M. Rafii, R. Elango, G. Courtney-Martin, J. D. House, L. Fisher, P. B. Pencharz, *Anal.Biochem.*, 2007, **371**, 71–81.
21 R. Saletti, S. Reina, M. Pittala, R. Belfiore, V. Cunsolo, A. Messina, D.V. Pinto, S. Foti, *Biochim. Biophys. Acta.*, 2017, **1859**, 301–311.
22 Y. V. Tcherkas, A. D. Denisenko. *J. Chromatogr A*., 2001, **913**, 309–313.
23 R. Glowacki, J. Stachniuk, K. Borowczyk, *Acta Chromatogr.*, 2016, **3**, 333–346.
24 M. Isokawa, T. Funatsu, M. Tsunoda, *Analyst,* 2013, **138**, 3802–3808.
25 J. X. Hong, W. Y. Feng, G. Q. Feng. *Sen. Actuat. B Chem.*, 2018, **262**, 837–844.
26 M. X. Li, W. Y. Feng, Q. S. Zhai, G. Q. Feng. *Biosens. Bioelectron.*, 2017, **87**, 894–900.
27 Q. Zhang, D. H.Yu, S. S. Ding, G. Q. Feng. *Chem. Commun.*, 2014, **50**, 14002–14005.
28 L. W. He, X. L.Yang, K. X. Xu, X. Q. Kong, W. Y. Lin. *Chem. Sci.*, 2017, **8**, 6257–6265.
29 Y. Qi, Y. Huang, B. Li, F. Zeng, S. Z. Wu. *Anal. Chem.*, 2017, **90**, 1014–1020.
30 M. Y. Jia, L. N. Niu, Y. Zhang, Q. Z. Yang, C. H. Tung, Y. F. Guan, L. Feng, *Acs. Appl. Mater Inter.*, 2015, **7**, 5907–5914.
31 T. Liu, F. J. Huo, J. F. Li, J. B. Chao, Y. B. Zhang, C. X. Yin, *Sen. Actuat. B Chem*., 2016, **237**, 127–132.
32 D. Z. Xu, M. Y. Liu, H. Zou, J. W. Tian, H. Y. Huang, Q. Wan, Y. F. Dai, Y. Q. Wen, X. Y. Zhang, Y. Wei, *Talanta,* 2017, **74**, 803–808.
33 M. Zhang, M. Yu, F. Li, M. Zhu, M. Li, Y. Ga, L. Li, Z. Liu, J. Zhang, D. Zhang, T. Yi, C. Huang, *J. Am. Chem. Soc.*, 2007, **129**, 10322−10323.
34 C. X. Yin, K. M. Xiong, F. J. Huo, James C. Salamanca, Robert M. Strongin, *Angew. Chem. Int. Ed.*, 2017, **56**, 13188–13198.
35 C. Yin, F. Huo, J. Zhang, R. Martínez–Máñez, Y. Yang, H. Lv, S. Li, *Chem. Soc. Rev.*, 2013, **42**, 6032−6059.
36 X. Y. Chen, P. Zhou, X. J. Yoon, *Chem. Soc. Rev.*, 2010, **39**, 2120−2135.
37 H. S. Jung, X. Chen, J. S. Kim, J. Yoon, *Chem. Soc. Rev.*, 2013, **42**, 6019−6031.
38 W. Wang, O. Rusin, X. Xu, K. K. Kim, J. O. Escobedo, S. O. Fakayode, K. A. Fletcher, M. Lowry, C. M. Schowalter, C. M. Lawrence, F. R. Fronczek, I. M. Warner, R. M. Strongin. *J. Am. Chem. Soc.,* 2005, **127**, 15949–15958.
39 Y. J. Wang, Z. R. Liu, G. M. Ren, X. Q. Kong, W. Y. Lin, *J. Mater. Chem. B*, 2017, **5**, 134–138.
40 Z. Y. Chen, Q. Sun, Y. H. Yao, X. X. Fan, W. B. Zhang, J. H. Qian, *Biosens. Bioelectron*. 2017, **91**, 553–559.
41 H. S. Jung, J. H. Han; T. Pradhan, S. Kim, S. W. Lee, J. L. Sessler, T. W. Kim, C. Kang, J. S. Kim, *Biomaterials*, 2012, **33**, 945−953.
42 X. Zhou, X. Jin, G. Sun, X. Wu, *Chem. Eur. J.*, 2013, **19**, 7817−7824.

View Article Online
DOI: 10.1039/C9NJ01259A

43 X. Yang, Y. Guo, R. M. Strongin. *Angew. Chem., Int. Ed*., 2011, **50**, 10690−10693.
44 Z. Guo, S. Nam, S. Park, J. Yoon, *Chem. Sci.*, 2012, **3**, 2760−2765.
45 B. Liu, J. Wang, G. Zhang, R. Bai, Y. Pang, ACS Appl. *Mater. Interfaces*, 2014, **6**, 4402−4407.
46 L. Y. Niu, Y. S. Guan, Y. Z. Chen, L. Z. Wu, C. H. Tung, Q. Z. Yang, *Chem. Commun*., 2013, **49,** 1294−1296.
47 R. Hu, J. A. Feng, D. H. Hu, S. Q. Wang, S. Y. Li, Y. Li, G. Q. Yang, *Angew. Chem. Int. Ed.*, 2010, **49**, 4915–4918.
48 D. P. Murale, H. Kim, W. S. Choi, D. G. Churchill, *Org. Lett.,* 2013, **15**, 3946–3949.
49 C. Huang, T. Jia, C. Yu, A. Zhang, N. Jia, *Biosens. Bioelectron*., 2015, **63**, 513–518.
50 O. Louant, B. Champagne, V. Liégeois, *J. Phys. Chem. A*., 2017, **122,** 972–984.
51 V. S. Padalkar, Y. Tsutsui, i. T. Sakura, D. Sakamaki, N. Tohnai, K. Kato, M. Takata, T. Akutagaw, K. I. Saka, S. Seki, *J. Phys. Chem. B.*, 2017, **121**, 10407−10416.
52 Y. C. Li, W. J. Di, Y. Yoon, *Sen. Actuat. B Chem.*, 2018, **259**, 347–353.
53 H. M. Lv , D. H. Yuan, W. P. Liu, Y. Chen, C. T. Au, S. F. Yin, *Sen. Actuat. B Chem.*, 2016, **233,** 173–179.
54 Q. Zhang, P. Zhang, Y. Gong, C. F. Ding, *Sen. Actuat. B Chem.*, 2019, **278,** 73–81.
55 P. Zhang, M. S. Zhu, H. Luo, Q. Zhang, L. E. Guo, Z. Li, and Y. B. Jiang, *Anal. Chem*., 2017, **89**, 6210−6215.
56 H. Sheng, Y. H. Hu, Z. C. Yi, S. Fan, C. Yang, X. X. Zhao, W. Yang, *Dye Pigment*, 2019, **160**, 48–57.
57 X. F. Yang, Y. X. Guo, R. M. Strongin. *Org. Biomol. Chem*., 2012, **10**, 2739-2741
58 X. F. Yang, Y. X. Guo, R. M. Strongin, *Angew. Chem. Int. Ed*., 2011, **50**, 10690–10693.
59 M. Zhang, L. Wang, Y. Zhao, F. Wang, J. L. Wu, *Anal. Chem.*, 2018, **90**, 4951-4954.
60 Y. Yue, Y. Guo, J. Xu, S. J. Shao, *New J. Chem.,* 2011, **35**, 61-64.
61 M. D. Weber, C. Garino, G. Volpi, E. Casamassa, M. Milanesi, C. Barolo, R. D. Costa, *Dalton Trans*., 2016, **45**, 8984–8993.
62 X. Yang, Y. Qian, *New J. Chem.,* 2019, **43**, 3725-3732.
63 S. Manna, P. Karmakar, S. S. Ali, U. N. Guria, R. Sarkar, P. Datta, D. Mandal, A. K. Mahapatr, *New J. Chem.,* 2018, **42**, 4951-4958.
64 N. Kundu, M. Maity, P. B. Chatterjee, S. J. Teat, A. Endo, M. Chaudhury, *J. Am. Chem. Soc.*, 2011, **50**, 20104–20107.
65 S. Park, O. H. Kwon, S. Kim, S. Park, M. G. Choi, M. Cha, S. Y. Park, D. J. Jang, *J. Am. Chem. Soc*., 2015, **127**, 10070–10074.

View Article Online
DOI: 10.1039/C9NJ01259A

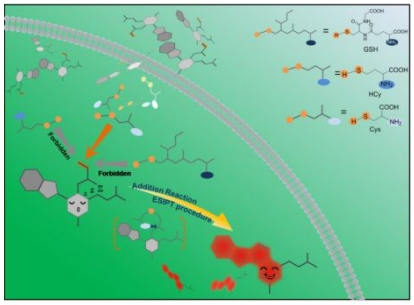

An HBT-based fluorescent probe for Cys with large Stokes shift and high selectivity was developed due to ESIPT process.